Thermal Hydraulic Investigation of EBR-II Instrumented Subassemblies during SHRT-17 and SHRT-45R Tests

Partha Sarathy U.[1], E. Bates[2], G. Su[3], A. Del Nevo[4], H. Ohira[5], H. Mochizuki[6], M. Stempniewicz[7], B. Truong[2], A. Moisseytsev[8] and T. Sumner[8]

[1]Indira Gandhi Centre for Atomic Research (IGCAR), Dept. of Atomic Energy, Kalpakkam, India

[2]TerraPower LLC, Bellevue, Washington, USA

[3]Xi'an Jiatong University (XIJU), Xi'an, Shaanxi, China

[4]Italian National Agency for New Technologies, Energy and Sustainable Economic Development, Brasimone, Italy

[5]FBR Plant Engineering Centre, Japan Atomic Energy Agency (JAEA), Tsuruga, Japan

[6]Research Institute of Nuclear Engineering, University of Fukui, Fukui, Japan

[7]Nuclear Research and Consultancy Group (NRG), Petten, Netherlands

[8]Argonne National Laboratory (ANL), Argonne, Illinois, USA

E-mail contact of main author: ups@igcar.gov.in

Abstract. The instrumented subassemblies XX09 and XX10 of EBR-II reactor were analyzed by various organizations using sub-channel/CFD codes as a part of the IAEA CRP project, 'Benchmark Analysis of an EBR-II Shutdown Heat Removal Test'. The XX09 was a 61 pin fuel subassembly and XX10 was an 18 pin non fuelled subassembly. Pins in both the subassemblies were wrapped by helical spacer wire. The geometry, initial steady state parameters, transient boundary conditions viz., decay heat generation rate, primary pump speed during coast down, IHX intermediate flow and inlet temperatures were supplied by ANL as input. The additional boundary conditions required for the subassembly analysis viz., the subassembly flow rate, inlet temperature, heat flux at the subassembly wrapper are obtained from the system analysis results. Because of the presence of spacer wire, the thermal hydraulics of the subassembly has become complicated. The simplified representation of the geometry could not capture the detailed flow and temperature distributions accurately. The CFD studies were found to be computational intensive and transient studies could not be continued for long duration. The sub-channel analyses gave reasonably good predictions with comparatively less computational requirements. The core top and SA top temperatures predicted by the sub-channel analysis codes and CFD codes are in reasonably good agreement with the measured values. The temperature distributions at the middle of the core predicted by CFD codes are in closer agreement with the measured values as compared to the predictions by sub-channel studies. The studies brought out the importance of thimble flow, inter-subassembly heat transfer, the effect of spacer wire and the power distribution inside the SA. This paper discusses about the modeling details of the SA with various codes and the comparison of the results with measured data.

Key Words: EBR-II, SHRT, CFD, Turbulence.

1. Introduction

Experimental Breeder Reactor (EBR-II) was a U-Pu-Zr metal-alloy fuelled liquid-metal-cooled fast reactor, extensively used for conducting safety experiments. EBR-II was heavily instrumented to measure sodium flows and temperatures at various locations in the primary circuit including the temperature distribution inside the subassemblies (SA). Several transient tests were conducted on the reactor to improve the understanding of thermal hydraulics and

neutronics of fast reactors. The shutdown heat removal tests (SHRT-17 & SHRT-45R) conducted in 1984 and 1986 demonstrated mechanisms by which fast reactors can survive severe accident initiators with no core damage. In order to utilize the data recorded during these tests and facilitate computer code validation, IAEA has initiated a coordinated Research Project (CRP), 'Benchmark Analyses of an EBR-II Shutdown Heat Removal Test' for benchmarking the SHRT-17 and SHRT-45R tests wherein 19 organizations representing eleven countries participated. Several participants simulated parts of the primary heat transport system using CFD codes. Amongst these studies, the sub-channel/CFD analysis of the instrumented SA (XX09 & XX10) are very important. XX09 was a 61-pin (59 fueled) SA with helically wound spacer wire over each pin and XX10 was a 19-pin non-fuelled SA. The instrumented SA are additionally cooled by a small amount of thimble flow around the SA. These SA were instrumented with wire wrap thermocouples, flow meters (below the core) and thermocouples at the SA inlet and outlet. A brief description of XX09 and XX10 SA geometry is given in the next section. More details about the geometry, initial conditions and the test procedure are given in the literature [1].

2. Instrumented SA

2.1 XX09 Subassembly

XX09 was a fueled subassembly containing 61 pin positions, of which 59 were driver fuel pins, and rest 2 were hollow tubes used as conduits to permit passage of instrument leads. The SA was located in 5th row. Two flow meters, one above the other, and two thermocouples were located at the subassembly inlet, and another 22 thermocouples were positioned at five axial locations. These were spacer wire thermocouples that replaced the standard spacer wires in 22 fuel elements. Thirteen of these thermocouples were located at the top of the core to give a two-dimensional radial temperature profile at that axial location. Two additional thermocouples recorded temperatures near the top of the control rod guide thimble that contained XX09. FIG. 1 shows the vertical section of the XX09 SA and vertical positioning of thermocouples and flow meters. FIG. 2 shows the plane cross-section of the SA and radial positioning of thermocouples. The combined instrumentation gave a detailed transient temperature and flow profile of the subassembly.

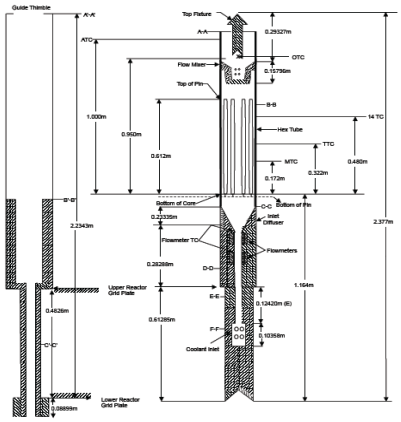

FIG.1. XX09 vertical section

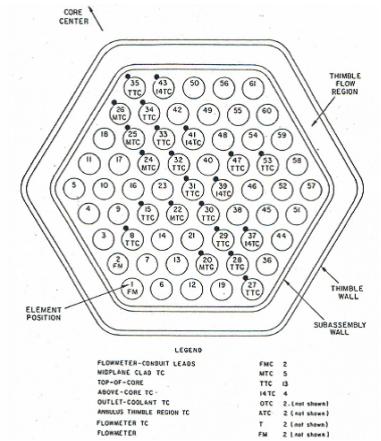

FIG. 2. XX09 instrumented subassembly thermocouple positions

2.2 XX10 Subassembly

XX10 was a non-fueled subassembly; like XX09, it was specifically designed with a variety of instrumentation to provide data for benchmark validation purposes. It contained 19 pin

positions, of which 18 were steel pins and one was a hollow tube used as a conduit to permit passage of instrument leads. The SA was located in a row 5. The subassembly instrumentation recorded data representative of a reflector subassembly. Two flow meters, one above the other, and two thermocouples were located at the subassembly inlet, and another 20 thermocouples were positioned at four axial locations. These were spacer wire thermocouples that replaced the standard spacer wires on all 18 pins. Seven of these thermocouples were located at the top of the core and seven at a location above the core, giving a two-dimensional radial temperature profile at both these axial locations. Two additional thermocouples recorded temperatures near the top of the control rod guide thimble. The combined instrumentation gave a detailed transient temperature and flow profile of the subassembly.

Table I: Design parameters of instrumented SA

Item	**XX09**	**XX10**
Number of elements	59 of 61	18
Clad outer / inner diameter	4.419/3.81 mm	8.81/0 (Solid rod)
Clad material	SS316	SS316
spacer wire diameter, mm	1.2446	1.2446
Spacer wire pitch, mm	152.4	152.4
Spacer wire material	SS316	SS316
Outer Hex tube Flat-to-flat outside, mm Flat-to-flat inside, mm Material	 58.17 56.1 SS304	 58.17 56.1 SS304
Inner Hex tube Flat-to-flat outside, mm Flat-to-flat inside, mm Material	 48.4 46.4 SS304	 48.4 46.4 SS304

3. Computational codes used

The organizations used different codes for investigating the multi-dimensional thermal hydraulic behaviour inside the XX09 and XX10 SA.

3.1 ANSYS CFX (ENEA)

ANSYS CFX [2] is a computational fluid dynamics code used for detailed three-dimensional analyses of fluid flow and (conjugate) heat transfer in the fluid and solid structures in both steady state and transient. The code employs a coupled technique that simultaneously solves all the transport equations in the whole domain through a false time-step algorithm. The linearized system of equations is reconditioned in order to reduce all the eigen values to the same order of magnitude. The multi-grid approach reduces the low frequency error, converting it to a high frequency error at the finest grid level; this results in a great acceleration of convergence.

3.2 ASFRE (JAEA)

This code is a sub-channel analysis code for SFRs and was also originally developed by JAEA for simulating thermal-hydraulics of wire-wrapped fuel pin bundles. This code has also

been validated by many sodium test facilities in Oarai. No open-literature documentation is available for this code.

3.3 COBRA4i (TerraPower, U. of Fukui)

The COBRA4i sub-channel methodology [3] decomposes a geometry (such as a rod bundle) into discrete sub-channels and then solves the coupled mass, momentum, and energy conservation equations to obtain the temperature and flow in each sub-channel. Flow redistribution between sub-channels is treated via the transverse momentum equation, while radial fluid conduction, azimuthal rod heat conduction, and forced mixing are treated using correlations[4].Transient analysis capability and use of the transverse momentum equation set the code apart from the other available sub-channel codes (e.g., SuperEnergy2). Forced mixing phenomena are treated in two ways: wire wrap sweeping and turbulent mixing. Heat transfer correlations specific to the coolant (sodium) are used to obtain cladding and fuel temperatures. The COBRA-4i code can be used for the analysis of water cooled reactor, liquid metal cooled reactor and gas cooled reactors. For liquid metal cooled fast reactors, the COBRA-4i code has been validated for the core and heat exchangers [5, 6].

3.4 STAR-CD (IGCAR)

STAR-CD[7] is a commercial computational fluid dynamics code which solves the governing differential equations of flow physics by numerical means on a computational mesh. It has the capability of solving steady, transient, laminar, turbulent, compressible, and incompressible flow phenomena along with heat transfer (conduction, convection and radiation) even in a porous medium. It has a built-in pre-processor and post-processor known as PROSTAR. It has a basic mesh generation capability. Complex meshes can be imported from any standard mesh generating tools. User-defined programme modules can be added to the code to modify the material properties as well as pressure drop and heat transfer characteristics dynamically during a transient. The code has been validated extensively against benchmark data.

3.5 TRACE (NRG)

The TRACE(TRAC-RELAP Advanced Computational Engine) code[8] is the latest in a series of best-estimate system codes developed by the U.S. Nuclear Regulatory Commission (NRC) for analysing steady-state and transient thermohydraulic-neutronic behaviour in light water reactors, as well as in advanced reactor systems cooled by helium, sodium or lead-bismuth eutectic. It can also model phenomena occurring in experimental facilities designed to simulate transients in reactor systems. Models used include multidimensional two-phase flow (single-phase flow for non-water fluids), non-equilibrium thermodynamics, generalized heat transfer, reflooding, level tracking and reactor kinetics, using either the point kinetics model or the PARCS 3D reactor kinetics solver integrated into TRACE.

4. Modeling Details and Results

4.1 ENEA

ANSYS CFX was used to model the XX09 instrumented SA (FIG. 3). It was geometrically built on the nominal sizing of the pin, the wire and the wrappers dimensions. A collapsed model was adopted for wires and pins simulation, avoiding the contact point issue involved in heat transfer phenomena. The model has 11.5 million nodes and 47.8 million elements. The

computational domain includes fuel pins, cladding, sodium region, inner hexagonal wrapper, sodium in the thimble region, outer hexagonal wrapper and the bypass fluid region simulated as a thin fluid region with symmetric boundary conditions on its external surfaces. Unstructured tetrahedral mesh elements were employed for all bodies of the model except for the fuel, where the elements were semi-structured. The working fluid is sodium, using RELAP5-3D© physical properties. The buoyancy effect in the sub-channels was neglected.

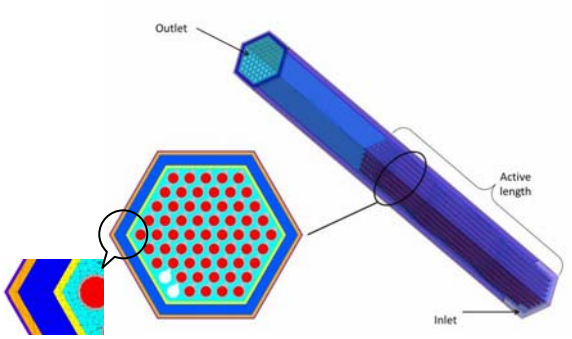

FIG.3. Computational mesh used

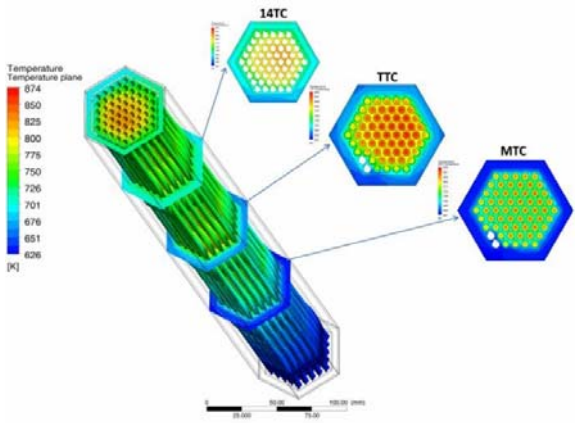

FIG. 4. Steady-state results for XX09

The multi-grid approach is followed to accelerated convergence. The turbulence is modeled using SST (Shear Stress Transport) k-ω model. The boundary conditions adopted are from the benchmark specifications and from the RELAP5-3D© simulation results (i.e. single-way coupling). The CFD model was based on a symmetric boundary condition on the external surfaces of the bypass region and asymmetric effects from the neighbouring fuel subassemblies were neglected. The simulation was limited to the first 100s of the test. FIG. 4 shows the steady state temperature distribution. The results show good agreement with the experimental values. Some differences still remain for the radial temperature profiles, due to asymmetric thermal behaviour of the neighbouring fuel subassemblies.

CFD results for the mid-core plane MTC in the transient simulation present good agreement with experimental results (FIG. 5), with a peak in the clad temperature of about 810 K at 65 s. There is a shift in time of 3-4 s on the maximum clad temperature prediction. Cladding temperatures at the top of the core plane (TTC) were in agreement with experimental results for t<45 s. Beyond 45 s, the maximum clad temperature was overestimated and showed a delay of about 10-15 s. In the mixing region, 14TC, the agreement with experimental data was good up to 70 s. After, there was an overestimation of the peak (60 K) and a delay (5 s).

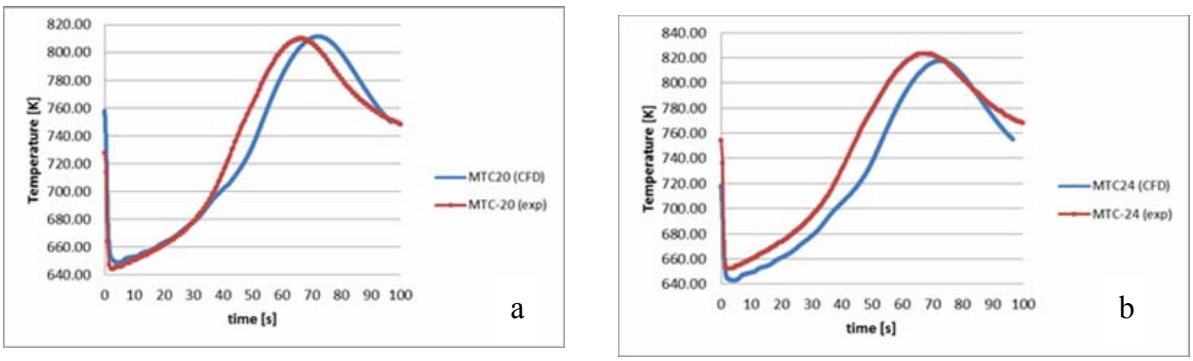

FIG.5. CFX XX09 cladding temperatures at the middle of the fuel bundle.

4.2 JAEA

The instrumented subassemblies XX09 and XX10 were simulated by using the ASFRE code. The SA inlet flow rate, inlet temperature and the heat flux at the SA wrapper as obtained from the system analysis results were given as boundary conditions. The coolant flow area in a subassembly was divided into sub-channels. The pressure drop in each sub-channel was described by Chang and Todreas's correlation. The heat transfer coefficient of the fuel pin bundle was described by Kazimi and Carelli's correlation [9].

FIG. 6 shows the sodium temperatures near the centre of the SA at the top (TTC) and middle (MTC) of the of the subassembly for XX09 and XX10 SA. In both cases, as can be seen, the numerical model tends to give predictions that are parallel to the measured temperatures. The simulated peak temperatures at the top of the core in XX09 and XX10 were underestimated by only 16 K and 9 K, respectively. It is seen that the simulated radial temperature distribution in XX09 has a parabolic shape initially at steady state and eventually flattens when natural circulation is established, similar to the behaviour of the measurements, while XX10 has a flat radial temperature shape throughout the transient because it is made of steel and has a low power density

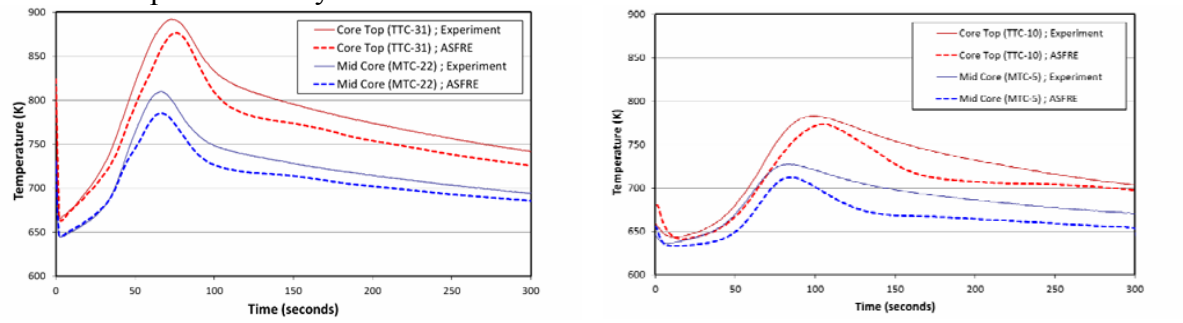

(a) ***(b)***

FIG. 6. Sodium temperatures near the centre of the subassembly at the top and middle of the core: (a) XX09, (b) XX10.

4.3 IGCAR

STAR-CD code was used to model the XX09 instrumented SA of SHRT-17 test. The geometry was modeled based on the nominal sizes of pin clad, spacer wire and SA wrapper. To avoid point contact between the clad and spacer wire, the circular spacer wire is modeled as wire with hexagonal cross-section and one edge of the hexagon touching the clad surface. The model has ~1 million computational volumes. The computational domain includes the fuel pin clad, the sodium surrounding fuel pins, the inner and outer hexagonal wrappers and the sodium in the thimble region. Complete structured mesh was generated using specialized grid generation software 'GRID-Z'. The buoyancy effect in the sub-channels was neglected. The SA inlet sodium flow rate and temperature as obtained from system analysis code were given as boundary conditions. The outer surface of the outer hexagonal wrapper is assumed to be adiabatic considering no inter-subassembly heat transfer. The steady state temperature at MTC and TTC elevations are compared with measured values in FIG. 9. The predictions are found to compare well with the measured data. Because of the heavy computational requirement, the transient analysis was carried out only for 100 s.

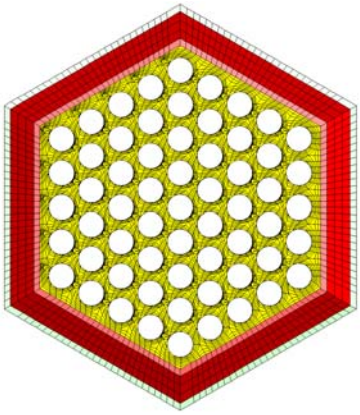

FIG. 7. Computational mesh used

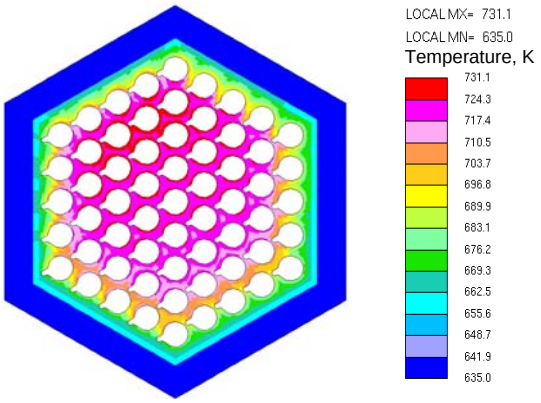

FIG. 8. Steady state temperature distribution at MTC thermocouple level

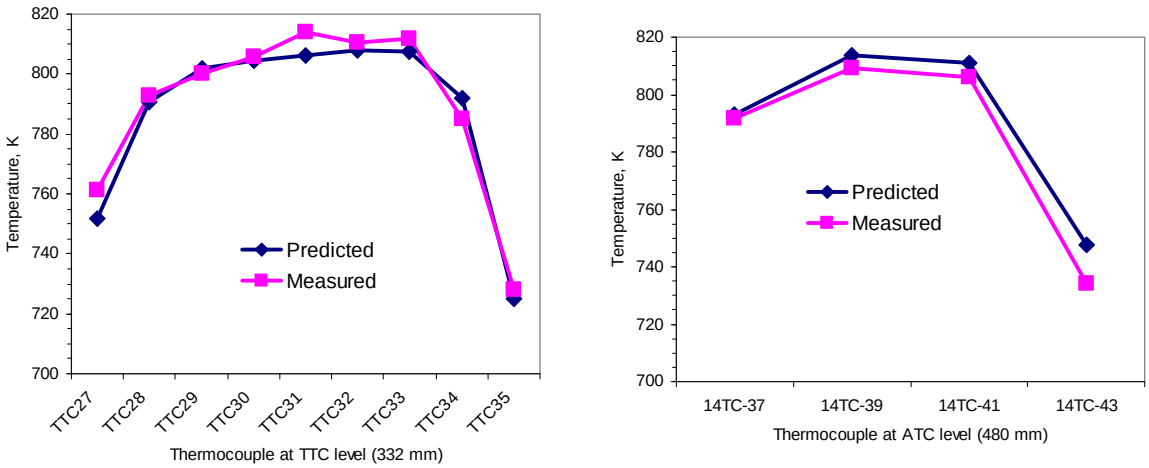

(a) *(b)*

FIG. 9. Steady state temperatures (Comparison with measured data)

4.4 NRG

The sub-channel analysis of XX10 SA was carried out with 48 PIPE-components, which all represent a sub-channel in either the internal subassembly, or the thimble region. The internal subassembly consists of the following sub-channels: 24 PIPEs represent the CENTRAL sub-channels; 12 PIPEs represent the edge sub-channels; 6 PIPEs represent the corner sub-channels. The remaining 6 PIPEs are used to represent the THIMBLE. In addition to the 48 PIPEs, the model consists also of: two lower plena (1 for the thimble, 1 for the subassembly); upper plenum, 102 HEATSTR which represent the steel rods (each facing a different sub-channel); 18 HEATSTR which represent the subassembly inner-walls (each facing a different sub-channel); 6 HS's representing the thimble walls (including the sodium gap for the neighbouring subassemblies); 924 side-junctions representing cross-flows within the subassembly and thimble. The code does not have a cross-flow model. FIG. 10 and FIG. 11 show the XX10 results obtained with the TRACE code, sub-channel model. The TRACE results show bigger channel-to-channel differences than does the measured data, because cross-flow mixing induced by spirally shaped wires was not taken into account by the code.

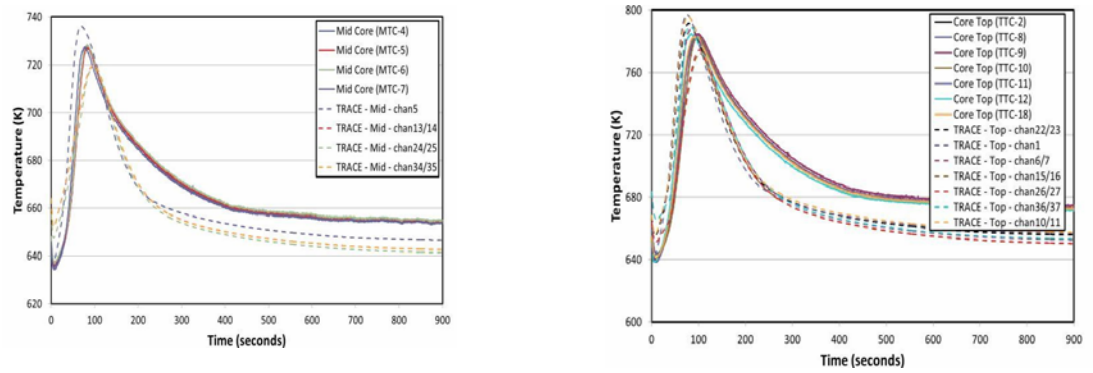

FIG. 10. SHRT-17, XX10 mid-core and top of the core temperatures – comparison with measured data

4.5 TerraPower

For calculating pin-level temperatures for the XX09 subassembly, the COBRA4i-MIT subchannel code (version 1.5) was used [10]. The SA inlet flow rate and temperature obtained from system analysis results were used as boundary conditions. FIG. 11 compares the SA outlet thermocouple predictions of phase-2 studies with measured data.

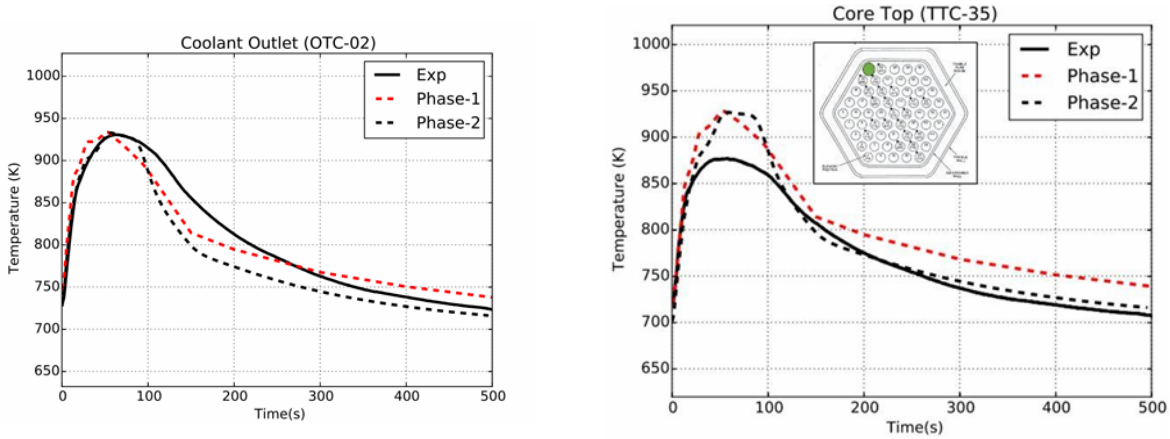

FIG. 11. Comparison of outlet and core top thermocouple temperatures from phase 2 studies with measured data.

Considering the uncertainties in the measured flow, flow distribution in the core, temperature measurements, decay heat data, the agreement between COBRA4i-MIT and the experimental results is good. Excluding the two outermost thermocouples (which are expected to have the greatest error due to wall effects that are not considered in COBRA4i-MIT), the error for temperature rise of the top of core thermocouples is within ±15% for the two time steps of interest.

4.6 U. of Fukui

For both SHRT-17 and SHRT-45R tests, the instrumented SA XX09 and XX10 were simulated using the COBRA-4i code. The SA inlet flow rate and temperature obtained from system analysis results were used as boundary conditions. The thermal capacity of the fuel was neglected. In SHRT-17 case, the effect of neutron flux gradient from the centre of the core to peripheral region on the power distribution amongst the fuel pins within the SA was considered. While in SHRT-45R case, the power tilt was not taken into account because of

the deployment situation around the XX09 SA. FIG. 182 shows the temperature distribution in XX09 SA of SHRT-17 test and compared with measured data. FIG. 12 shows the temperature distribution in the cross-section at TTC elevation. It can be seen that without spacer wire the temperature distribution is flatter than that with spacer wire. With spacer wire the predictions are better in the region away from centre of the core (TTC-27 to 31) than in the region closer to the centre of the core (TTC-31 to 35).

FIG. 13 shows the evolution of TTC-31 thermocouple temperature of SHRT-45R test predicted by COBRA-IV-I code and its comparison with measured data. It can be seen that during first 200 s the temperatures are under predicted, while the temperatures at later time are over predicted. It is seen that the predicted temperatures at the top of the XX09 SA matches the measured temperature well except in the tail region, at the end of the transient It is also seen that all the predicted temperatures are closer to the measurements except TTC-35. A difference between the SHRT-17 and SHRT-45 test is sharpness of the power transient. In the case of SHRT-45R, the power transient rate is slightly milder than for SHRT-17. Therefore, it is estimated that the heat capacity and heat conduction have only a small effect on the temperature transient. Radial temperature profiles during the transient were predicted reasonably well.

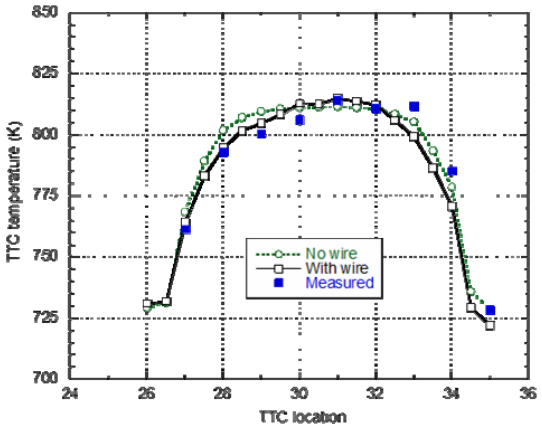

FIG. 12. Comparison of the COBRA-IV-I predictions at core top in XX09 SA of SHRT-17 test with measured data

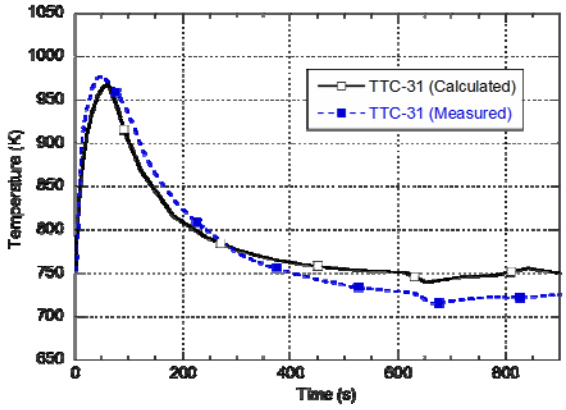

FIG.13. Comparison of COBRA-IV-I predictions at core top in XX09 SA of SHRT-45R test with measured data

4.7 ANL

XX09 and XX10 instrumented subassemblies and their six neighbouring subassemblies were modelled using the SAS4A/SASSYS-1 sub-channel model with total 2448 channels for 14 SA. FIG. 14 compares the predicted temperature of the TTC-31 thermocouple of SHRT-17 test with the measured data. FIG. 15 compares the predicted temperature of TTC-31 thermocouple of SHRT-45R test with the measured data. It can be seen that the predictions are reasonably good.

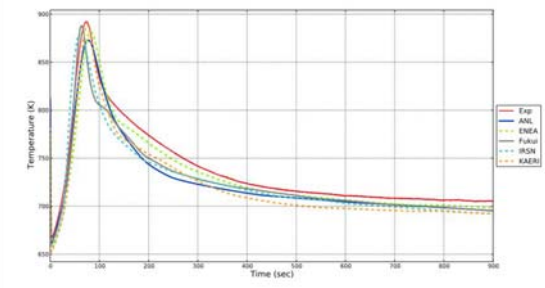

FIG. 14. Comparison of TTC-31 temperature of SHRT-17 test with measured data

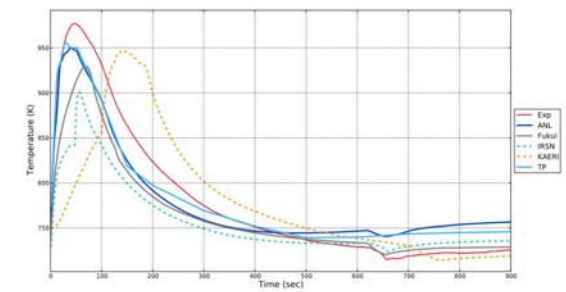

FIG. 15. Comparison of TTC-31 temperature of SHRT-45R test with measured data

5. Conclusion

The thermal hydraulics of instrumented SA is found to be complicated because of the spacer wire and the inter-subassembly heat transfer. The CFD studies were found to be computationally intensive and transient studies could not be continued for long duration. The sub-channel analyses gave reasonably good predictions with comparatively less computational requirements. The core top and SA top temperatures predicted by the sub-channel analysis codes and CFD codes are in reasonably good agreement with the measured values. The temperature distributions at the middle of the core predicted by CFD codes are in closer agreement with the measured values as compared to the predictions by sub-channel studies.

6. References

[1] SUMNER, T. and WEI, T., Benchmark Specifications and Data Requirements for EBR-II Shutdown Heat Removal Tests SHRT-17 and SHRT-45R, ANL-ARC-226, Rev. 1, Argonne National Laboratory, Argonne, Illinois (2012).

[2] ANSYS CFX Release 15.0 User Manual, ANSYS, Inc. (2013).

[3] WHEELER, C.L.,*et al.*,COBRA4i Code System to Calculate Rod-bundle and Core Thermal-Hydraulics, BNWL-1962, Battelle Pacific Northwest Laboratories, Richland, WA, USA(1976).

[4] FRICANO, J. and BUONGIORNO, J., "COBRA4i-MIT: an Updated Sub-Channel Analysis Code for Sodium Fast Reactor Design," in International Congress on Advances in Nuclear PowerPlants (ICAPP), Nice, France(2011).

[5] DONOVAN, T.E., GEORGE, T.L., and WHEELER, C.L., COBRA-IV Wire Wrap Data Comparisons, Pacific Northwest Laboratory, PNL-2938 (1979).

[6] BOGOSLOVKAYA, G. P., CEVOLANI, S., and NINOKATA, H., LMFR Core and Heat Exchanger Thermohydraulic Design: Former USSR and Present Russian Approaches, IAEA-TECDOC-1060, IAEA, Vienna (1999).

[7] STAR-CD, version 3.26, Computational Dynamics, Ltd., New York, USA, 2005.

[8] U. S. NUCLEAR REGULATORY COMMISSION, TRACE V5.840 User's Manual, Volume 1: Input Specification, Volume 2: Modeling Guidelines(2014).

[9] KAZIMI, M. S. and CARELLI, M. D., Heat Transfer Correlation for Analysis of CRBRP Assemblies, CRBRP-ARD-0034, Westinghouse (1976).

[10] BATES, E., *et al.*, "Phase 2 of the EBR-II SHRT-45R benchmark study – TerraPower's COBRA-4i-MIT results", International Congress on Advances in Nuclear Power Plants (ICAPP) San Francisco (2016).